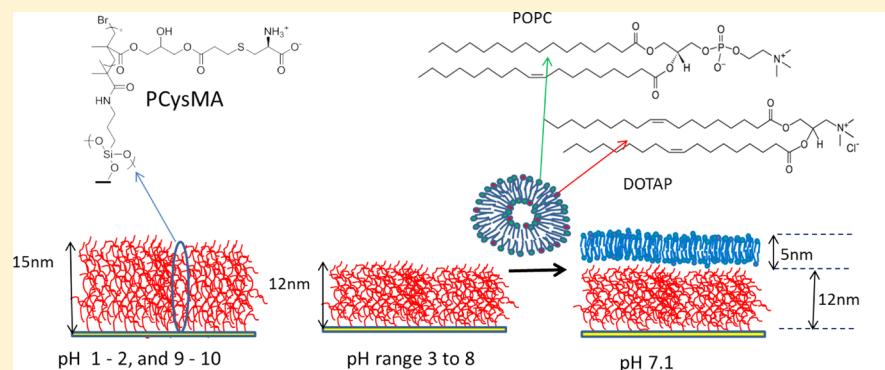# Langmuir

New Poly(amino acid methacrylate) Brush Supports the Formation of Well-Defined Lipid Membranes

Anita C. Blakeston,[†] Abdullah M. Alswieleh,[‡] George R. Heath,[†] Johannes S. Roth,[†] Peng Bao,[†] Nan Cheng,[‡] Steven P. Armes,[‡] Graham J. Leggett,[‡] Richard J. Bushby,[†] and Stephen D. Evans*,[†]

[†]Molecular and Nanoscale Physics Group, School of Physics and Astronomy, University of Leeds, Leeds LS2 9JT, United Kingdom
[‡]Department of Chemistry, University of Sheffield, Sheffield S3 7HF, United Kingdom

Ⓢ Supporting Information

ABSTRACT: A novel poly(amino acid methacrylate) brush comprising zwitterionic cysteine groups (PCysMA) was utilized as a support for lipid bilayers. The polymer brush provides a 12-nm-thick cushion between the underlying hard support and the aqueous phase. At neutral pH, the zeta potential of the PCysMA brush was ∼−10 mV. Cationic vesicles containing >25% DOTAP were found to form a homogeneous lipid bilayer, as determined by a combination of surface analytical techniques. The lipid mobility as measured by FRAP (fluorescence recovery after photobleaching) gave diffusion coefficients of ∼1.5 $\mu m^2\ s^{-1}$, which are comparable to those observed for lipid bilayers on glass substrates.

■ INTRODUCTION

Lipid membranes, and the proteins incorporated within them, have been the focus of significant research effort in recent years, mainly because of their importance in signal transduction and the control of cell function.[1−4] From their inception, planar-supported lipid bilayers (SLBs) have provided useful model systems for studying (i) the role of membrane composition, (ii) the function of membrane proteins in 2D systems, and (iii) ion-channel-based sensors.[5−9] A range of strategies have been explored for forming planar lipid membrane systems, including electrostatic interactions for supported lipid bilayers,[10,11,18] the insertion of anchoring units in the formation of tethered lipid bilayers (TLBs),[12−17] and lipid monolayer adsorption at hydrophobic surfaces for the formation of hybrid lipid bilayers (HLBs).[18] For the incorporation of fully functional membrane proteins, it is desirable to have a "spacer" region between the bilayer and the underlying solid support to prevent the protruding extremities of the membrane protein from interacting directly with the surface.[19,20] Most SLBs and TLBs produce bilayers separated from the surface by a thin water layer of 0.5 to 1.0 nm thickness,[21] i.e., much thinner than typical extra-membranous protein regions. Therefore, routes to provide thicker aqueous/gel-like supports for lipid bilayers have been the subject of significant research. In principle, protein-resistant hydrophilic polymers could provide a solution to this problem by presenting a hydrated support that would interact minimally with any incorporated (trans-membrane) protein while providing a support for bilayer formation. The underlying hydrated polymer brush would also provide a suitable "reservoir" to allow the diffusion of ions and small molecules.

A number of strategies have been explored to provide polymeric supported lipid bilayers. Lipo-polymer anchors in which a polymer "cushion" is chemically attached to the solid surface and also has lipid moieties that insert into the proximal leaflet of a lipid bilayer to anchor it to the surface have been examined by a number of groups.[22−26] Notably, Mashaghi et al. reported a method based on the spin-coating of lipids onto a lipopolymer-PEG brush, providing a spacing of several nanometers, followed by the fusion of protein-containing vesicles with the SLB.[27]

Alternative polymer supports have included biopolymers such as dextran or cellulose as spacers. Using cellulose allowed the formation of functional bilayers using vesicle adsorption,[28]

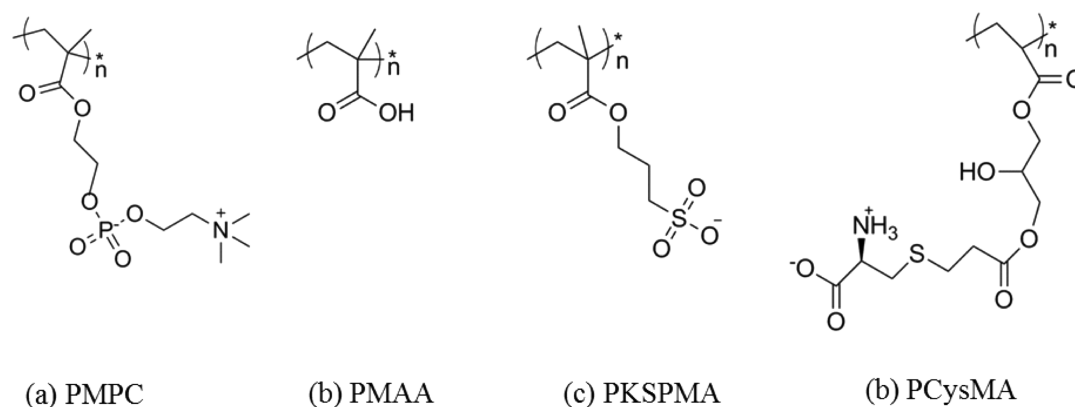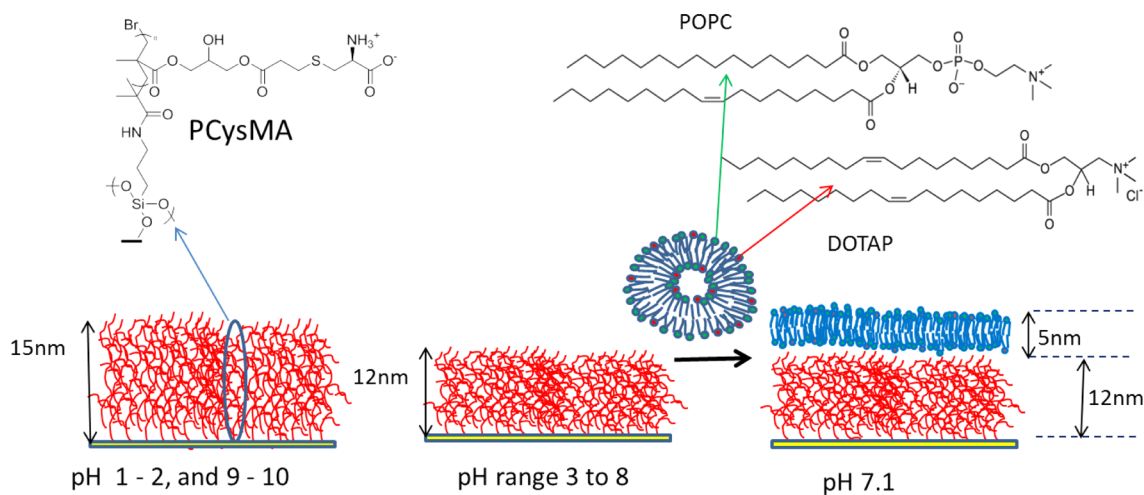(a) PMPC   (b) PMAA   (c) PKSPMA   (b) PCysMA

Figure 1. Chemical structures of the four polymer brushes explored as potential lipid bilayer supports.

Scheme 1. (Left) Schematic Representation of the pH-Responsive Poly(cysteine methacrylate) (PCysMA) Brush Grown from a Planar Glass Surface[a] and (Right) the POPC/DOTAP Lipid Binary Mixture Used to Form the Bilayer on the PCysMA Brush at pH 7

[a]The PCysMA brush (dry thickness = 5−8 nm) has a hydrated thickness of 15−24 nm below pH 3 and above pH 8. Between pH 3 and pH 8, the brush has an average thickness of 12 nm.

but dextran required Langmuir−Blodgett deposition for DMPC bilayer formation.[29]

Finally, there are a number of literature examples of the use of neutral, zwitterionic, or polyelectrolyte brushes as supports for lipid bilayers. In addition to using zwitterionic or neutral polymer brushes, it is possible to use electrostatic interactions as the driving force for bilayer formation. For example, Smith et al. formed POPC lipid bilayers via vesicle adsorption onto polyacrylamide (PAM) brushes grown by atom-transfer radical polymerization (ATRP) and found lipid diffusion coefficients ($\sim$2 μm^2 s^{-1}) similar to those obtained for bilayers on glass. Interestingly, they attribute their ability to form bilayers on these surface as due to the exceptional smoothness (rms roughness <0.5 nm) of the brush layer produced by ATRP; in contrast, spin-coated PAM films (rms roughness $\sim$3 nm) did not support bilayer formation.[30] Vancso et al. grew zwitterionic sulfobetaine polymer brushes (PSBMA) via surface ATRP and found that (DOPC) bilayer adsorption could be tuned by controlling the grafting density/polymer thickness. No bilayer formation was obtained for swollen brush thicknesses greater than 35 nm, while bilayers formed on $\sim$16 nm brushes gave lipid diffusion coefficients on the order of 1 μm^2 s^{-1}.[31] A maleic anhydride-based, pH-responsive brush developed by Renner

and coworkers supported bilayer formation if electrostatic repulsion was reduced by lowering the pH to 4. Three brushes of 4, 25, or 60 nm dry thickness were examined, which led to bilayers with diffusion coefficients of 0.26, 0.60, or 1.24 μm^2 s^{-1}, respectively. They also successfully incorporated a functioning transmembrane protein (BACE) which displayed enhanced activity when the protein was incorporated into the brush-supported bilayer.[32] A pH-responsive hydrophilic cushion of poly(acrylic acid) (PAA) was utilized by El-Khouri et al., who used LB/LS deposition to prepare neutral bilayers that enabled rapid lipid diffusion at pH 9.[33]

Cationic poly(diallyldimethylammonium chloride) grafted to a planar surface has been used by Tang et al. to support a bilayer formed on highly anionic vesicles. At around 60% anionic DOPG lipid and low or zero ionic strength, a smooth bilayer was formed, as determined by AFM and QCMD.[34] Similarly, a weakly anionic polyelectrolyte brush based on a copolymer comprising N-isopropylacrylamide and acrylic acid has also been used as a membrane support.[35] In this case, a bilayer was formed from a 1:9 cationic/zwitterionic lipid binary mixture using a dehydration/rehydration protocol, yielding bilayers with diffusion coefficients of between 6 and 9 μm^2 s^{-1}, roughly twice that found for glass. Alternating layers of

polyelectrolytes allow specific properties to be designed into the polymer support. Fischlechner et al. employed polyelectrolyte multilayers composed of a cationic (PAH) upper layer and an anionic (PSS) lower layer. This approach enabled successful bilayer formation when using a 50:50 mixture of zwitterionic and anionic lipids POPC and POPS (1-hexadecanoyl-2-(9Z-octadecenoyl)-sn-glycero-3-phopho-L-serine (sodium salt). Other combinations of purely anionic or purely zwitterionic lipids produced adsorbed vesicles, but these remained intact, rather than fusing to form a homogeneous bilayer.[36]

The main requirement for such polymer supports is that they should facilitate the formation of defect-free lipid bilayers that enable the incorporation of fully functional transmembrane proteins (TMPs) as the conduit for charge/ion movement across the membrane. Ideally, the TMP should not interact strongly with either the solid support or the polymer brush. The polymer brush should be of controlled thickness, have a uniform and sufficiently high grafting density, possess minimal surface roughness, and should be chemically attached to the solid support. The ATRP approach employed in this work allows good control of the chain growth kinetics and hence the mean brush thickness.[37−39] As the design rules for a suitable choice of polymer brush are not yet fully understood, we investigated four candidates: poly(cysteine methacrylate) (PCysMA)[46] and poly(2-(methacryloyloxy)ethyl phosphorylcholine) (PMPC)[40] zwitterionic brushes plus poly(methacrylic acid) (PMAA)[41] and poly(potassium 3-sulfopropyl methacrylate) (PKSPMA) anionic brushes (Figure 1).

All polymer brushes were grown from glass substrates using surface ATRP. Comparisons of bilayer formation were made using vesicles of varying lipid composition through the addition of cationic lipid to drive the electrostatic interaction with the polymer brush. Fluorescence recovery after photobleaching (FRAP) was used to evaluate bilayer quality, and in cases in which bilayer formation was observed, atomic force microscopy (AFM) was used to establish height profiles for both the polymer brush and the lipid bilayer and also to perform breakthrough force measurements.

■ EXPERIMENTAL SECTION

Polymer Brush Synthesis and Characterization. The four polymer brushes (PCysMA, PMPC, PMAA, and PKSPMA) examined in this work were grown from planar glass surfaces using ATRP, and the structures for these are shown in Figure 1. First, a 3-aminopropyltriethoxysilane (APTES) silane layer was adsorbed from ethanol to provide a suitable amine surface. This was then reacted with 2-bromoisobutyryl bromide (BIBB, 0.37 mL, 3 mmol) and triethylamine (0.41 mL, 3.0 mmol) in 60 mL of dichloromethane (DCM) for 30 min.[42] These initiator-functionalized surfaces were subsequently reacted with the relevant brush monomers, as described previously.[43−47] All brush layers were characterized by a combination of AFM, XPS, and ellipsometry. For the work described herein, dry brush thicknesses were 5−9 nm.

Materials. The lipids used for this study were POPC (1-palmitoyl-2-oleoyl-sn-glycero-3-phosphocholine) and DOTAP (1,2-dioleoyl-3-trimethylammonium-propane), both of 99% purity and obtained from Avanti Polar Lipids (Alabaster, AL). These lipids are fluid at room temperature and have transition temperatures of just below 0 °C. Texas red DHPE (1,2-dihexadecanoyl-sn-glycero-3-phosphoethanolamine triethylammonium salt, Invitrogen) was used as a fluorescent probe. The dried lipids were used as received and dissolved in a 50:50 mixture of HPLC-grade chloroform and methanol prior to transfer into glass vials in the following molar ratios: 99.5:0.5 POPC/Texas red (subsequently denoted as POPC), 10:89.5:0.5 DOTAP/POPC/Texas

red (denoted as 10% DOTAP), 24.9:74.6:0.5 DOTAP/POPC/Texas red (denoted as 25% DOTAP), and 49.75:49.75:0.5 DOTAP/POPC/Texas red (denoted as 50% DOTAP). The solvent was removed by drying the lipid under a flow of nitrogen gas for 1 h. Once fully dry, the lipids were hydrated using a phosphate buffer, which is a 10 mM mixture of sodium dihydrogen phosphate and disodium hydrogen phosphate in Milli-Q water (18.2 MΩ cm^{-2} MilliPore Ltd, Watford, U.K.) adjusted to pH 7.1 with NaOH or HCl. The same buffer was used for ionic strength experiments but with the addition of NaCl to achieve the required molarity (up to 140 mM). HCl was obtained from Fisher Scientific, and all other chemicals were purchased from Sigma-Aldrich.

Vesicle solutions were prepared at a concentration of 1.0 mg mL^{-1} by vortex mixing the lipid solution for 1 min at maximum speed (Vortex Genie2, Jencons Ltd., Leighton Buzzard, U.K.) to create multilamellar vesicles as a cloudy suspension. Small unilamellar vesicles (SUVs) were prepared by tip sonication (Branson Sonifier 750, Branson Ultrasonics Corp., Danbury, CT) of the suspension at 4 °C for 20 min, during which time the suspension became clear. The suspension was centrifuged (Heraeus Fresco 17, Thermo Fisher Scientific, Loughborough, UK) for 1 min at 14 500g, after which the supernatant was removed and retained. The suspension was diluted with buffer to 0.5 mg mL^{-1} prior to use and stored at 4 °C in the dark for no longer than 5 days.

Surface Preparation. The 18-mm-diameter round glass coverslips (VWR International Ltd., U.K.) used for studying bilayer diffusion were cleaned by sonication in a 2% Decon-90 solution (Decon Laboratories Ltd., Hove, U.K.). These slides were then rinsed with Milli-Q water, sonicated with water, and sonicated again with propan-2-ol (ultrasonic bath for 10 min). Finally, they were rinsed extensively with Milli-Q water and cleaned using a piranha solution (a mixture of 30% hydrogen peroxide and 70% sulfuric acid) for 5 min. Polymer brushes were grown from these coverslips, and immediately before bilayer formation experiments, the polymer brushes were rinsed with propan-2-ol and Milli-Q water with a further brief period of sonication. All samples were dried under a flow of nitrogen gas.

Supported Lipid Bilayer Formation. Bilayer formation on bare glass (controls) and the polymer brush-coated glass took place in a custom-built flow cell. For bare glass substrates, the vesicles were injected and incubated for 1.0 h at 22 °C. The samples were subsequently rinsed for 20 min with degassed Milli-Q water at a flow rate of 2.6 mL min^{-1}. For the brush-coated surfaces, the samples were first soaked with buffer solution for 10 min, followed by injection with vesicles at 22 °C before a subsequent incubation for 1 h at 50 °C in the dark. The samples were subsequently rinsed for 20 min with degassed Milli-Q water at a flow rate of 2.6 mL min^{-1}. FRAP studies were then conducted. Samples for which an immobile bilayer or an incompletely formed bilayer was observed were incubated for another 48 h at 22 °C, rinsed, and imaged again. The bilayers were checked for stability after 5 days of storage at 22 °C.

Bilayer Characterization. The incorporation of fluorescent probes into the lipid vesicles enabled the use of fluorescence microscopy to study bilayer fluidity. FRAP was assessed using an epifluorescence microscope (E600 Nikon, USA). The sample was illuminated and bleached by a high-pressure mercury arc lamp. The bleached spot radius was 14 μm when using a 40× objective lens. Fluorescence images were collected using Zyla sCMOS CCD (Andor Technology Ltd., Belfast, U.K.) with 2 × 2 binning and recorded on NIS elements software. Images were collected until complete fluorescence recovery was observed. The Axelrod method of analysis was employed, which provides both the diffusion coefficient and the mobile fraction.[48]

Size and Zeta Potential Characterization of Lipid Vesicles. These parameters were determined using a Zetasizer Nano ZS instrument (Malvern Instruments, Malvern, U.K.) at 25 or 50 °C equipped with a folded capillary cell (DTS 1060 or 1070). The detection angle was 12°, and the particle mobility was converted into zeta potential using the Smoluchowski approximation.[49] Three measurements were made on each of the samples, and data were averaged. The intensity-averaged hydrodynamic diameter was also
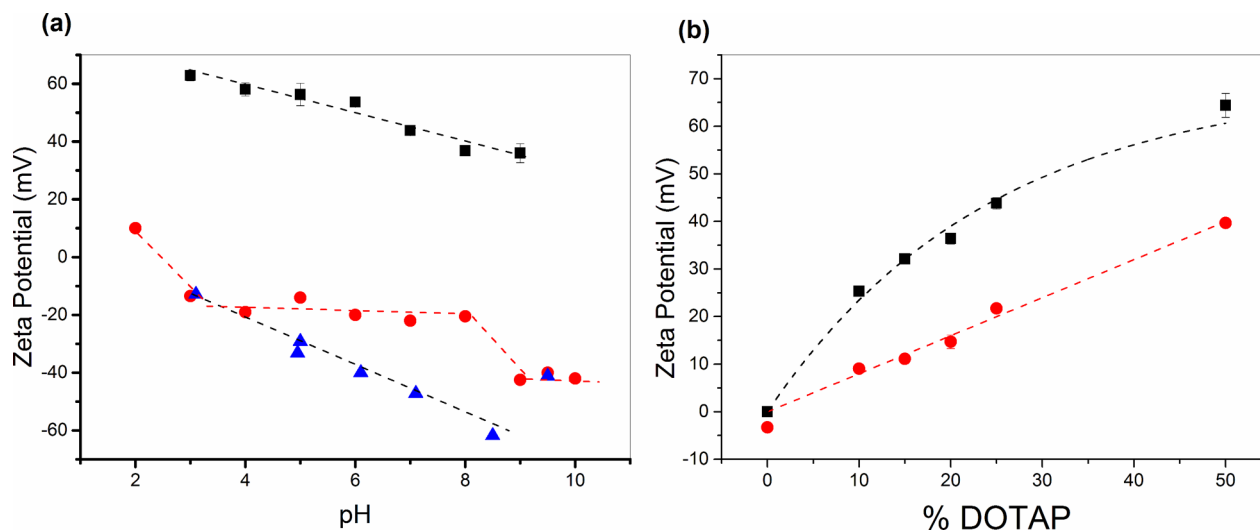
(a) **(b)**

Figure 2. (a) Zeta potential data obtained for the DOTAP/POPC (25:75) lipid vesicles (black squares) and the PCysMA brush (red circles) as a function of pH. Data for a clean glass surface (blue triangles) for comparison. (b) Zeta potential data for vesicles of varying DOTAP/POPC molar ratios in phosphate buffer at pH 7 (black squares) and in the presence of 140 mM NaCl (red circles). The dotted lines provide a guide to the eye.

determined in all cases to assess the colloidal stability of the lipid vesicles. The effect of elevated temperature (used for the incubation of lipids on the brushes) was examined by maintaining the lipid vesicles in the zeta cell at 50 °C for 1 h and then repeating the zeta potential and particle size measurements. The vesicle size measurements utilized dynamic light scattering at a detection angle of 173° (with three measurements being recorded per sample). The least-squares algorithm was used within the instrument software to analyze the data.

Zeta potentials of the bare glass and polymer-brush-coated glass substrates were determined using a Zetasizer Nano dip cell (ZEN 1020), which is used in conjunction with the Zetasizer Nano ZS instrument. The dip cell holds a small, flat sample (4 mm × 7 mm) of the planar surface of interest. Measurements were recorded at 25 and 50 °C using a 0.01% aqueous dispersion of a nonadsorbing sterically stabilized polystyrene latex in 1 mM KCl as the tracer particles. Zeta potential measurements were recorded at various positions (125, 250, 375, 500, and 1000 μm) from the planar substrate. The electrophoretic motion is constant across this distance range, whereas the electro-osmotic effect is reduced with distance from the surface, to a point (at 1000 μm) where only electrophoretic behavior is observed.

AFM. All AFM images and measurements of the breakthrough force were made at 22 °C using a Bioscope AFM instrument equipped with a NanoScope III controller (Bruker Daltonics, Billerica, MA) and an inverted wide-field Axiovert 200 fluorescence microscope (Carl Zeiss, Inc., Thornwood, NY). Oxide-sharpened silicon nitride tips were used in tapping or contact mode with a spring constant of 0.32 N m^{-1}, and all images were recorded on PCysMA-coated glass substrates before and after bilayer formation.

^{1}H NMR Spectroscopy. A 2.0% w/w aqueous solution of PCysMA$_{30}$ homopolymer (mean degree of polymerization = 30) was heated to 50 °C at pH 7 in D$_2$O. Spectra were recorded over a 2 h period to examine whether hydrolytic degradation occurred under these conditions.

■ RESULTS

Four different brush-functionalized surfaces were fabricated and evaluated as potential supports for lipid bilayer formation. The PMPC and PCysMA brushes are zwitterionic at neutral pH, and the PMAA and PKSPMA brushes are both highly anionic under these conditions. Dry brush thicknesses of 5−9 nm, which swell 2- or 3-fold when hydrated in buffer, were used to provide an aqueous region beneath the bilayer so as to act as a reservoir for ions and, in future work, to accommodate the extra-membranous portions of membrane proteins. The

synthesis and characterization of these brushes has been recently described in detail.[44,50]

Zeta Potential of the Polymer Brushes. The surface zeta potential for both PCysMA and a planar glass substrate control was determined as a function of pH (Figure 2a).[46] The zwitterionic PCysMA (red circles) brushes displayed a weakly negative surface zeta potential of −10 ± 5 mV between pH 3 and pH 8, whereas the PMPC brush exhibited a surface zeta potential of ∼0 ± 10 mV.[44] For comparison, bare glass (blue triangles) exhibited a linear reduction in surface zeta potential from −12 to −60 mV with increasing pH. The anionic PMAA and PKSPMA brushes displayed zeta potentials close to those of glass at pH 7 (−43.2 ± 1.5 vs −33.6 ± 2.3 mV, respectively). The latter data are consistent with values reported for PMAA-coated nanoparticles, which displayed a zeta potential of ∼−35 mV at or above pH 6,[51] and PKSPMA-coated nanoparticles, which displayed highly negative zeta potentials (∼−50 mV) with essentially zero pH dependence over the pH range considered here.[52]

DLS and Zeta Potential Studies of Vesicles. POPC-based vesicles containing increasing amounts of DOTAP were formed by tip sonication in phosphate buffer at pH 7 and 25 °C. There was no significant size dependence on composition, with the average vesicle diameter being 27 ± 2 nm. There was a slight increase up to 30 ± 1 nm diameter upon incubation at 50 °C. The zeta potential increased almost linearly with DOTAP concentration from ∼0 mV for pure POPC vesicles up to around +60 mV for a 1:1 mixture of POPC/DOTAP (Figure 2b). For a given vesicle composition, the zeta potential increased at lower pH and was reduced upon addition of salt. The zeta potential of pure POPC lipids has been previously shown by Cho et al. to vary between −1 and −10 mV from pH 4 to pH 9, respectively.[53]

Lipid Bilayer Formation. Attempts to form bilayers via the incubation with small unilamellar vesicles (SUVs) comprising pure POPC failed for each of the four polymer brushes, although the same strategy proved to be successful for glass surfaces. Because two of the polymer brushes were anionic (with surface zeta potentials of approximately −40 to −50 mV, i.e., in the same range as glass), this failure to yield bilayers suggests that the chemical structure of the polymer cushion and
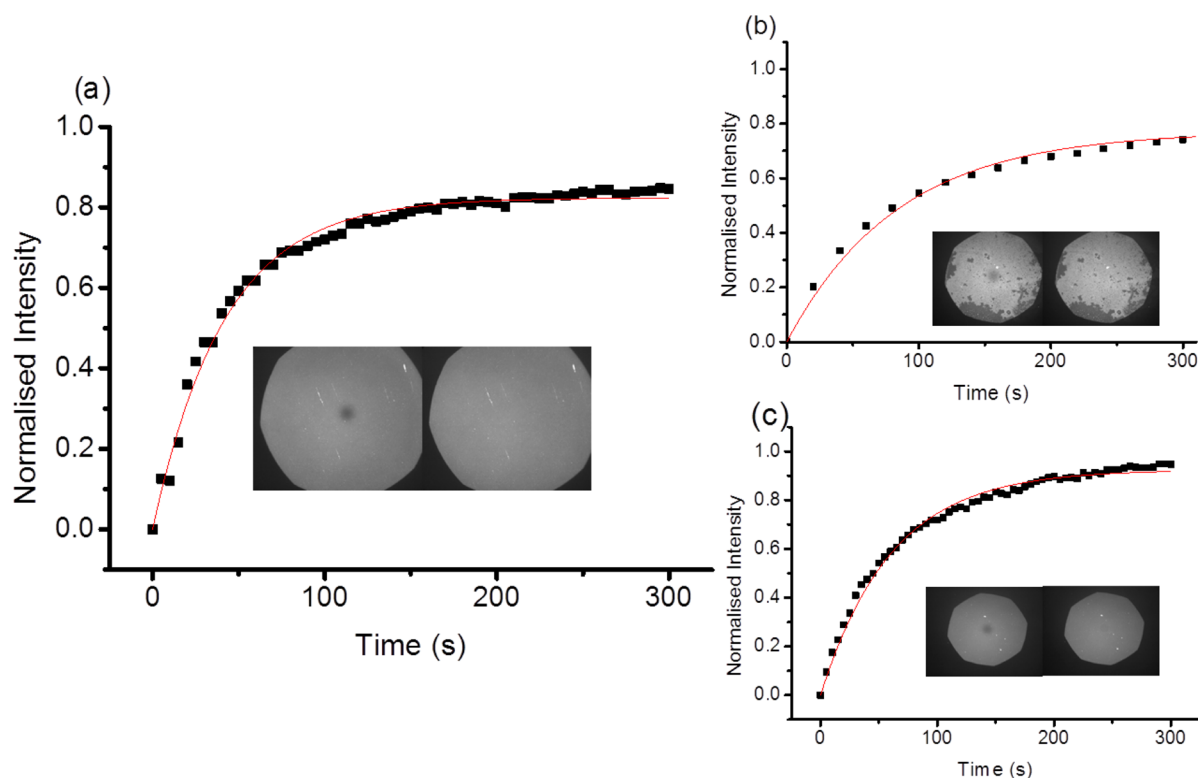
Figure 3. Fluorescence recovery after photobleaching (FRAP) curves recorded for (a) a fluid bilayer on a PCysMA brush formed after full incubation; (b) a double bilayer adsorbed on a PCysMA brush (dry thickness 5−8 nm) following incubation at 50 °C for 1 h; and (c) a single bilayer formed after 48 h of incubation at 20 °C for the sample shown in (b). The vesicles comprised 25% DOTAP, 75% POPC, and 0.5 mol % Texas red in 10 mM phosphate buffer at pH 7.

its associated water layer must play an important role in bilayer formation (or its prevention). In general, while some isolated vesicle adsorption was observed on these brushes, this was only at very low surface coverage. Because all of the surfaces exhibit either a zero, slightly negative, or substantially negative surface zeta potential, the effect of incorporating cationic lipids into the liposomes was investigated. Accordingly, SUVs comprising 10, 25, and 50 mol % cationic lipid (DOTAP) and POPC were prepared for evaluation.

Bilayer Formation on PMPC and PCysMA. For the PMPC brushes, little or no vesicle adsorption was observed for any of the vesicle compositions used. For the PCysMA brushes, it was found by using 10% DOTAP that some SUVs were absorbed but again only at relatively low surface coverage. Increasing the DOTAP concentration to 25 mol % produced a dense layer of adsorbed vesicles, but bilayer formation was not observed. However, on raising the temperature to 50 °C for 1 h, followed by rinsing and another 48 h incubation period at room temperature, a high-quality bilayer could be formed, as evidenced from the FRAP data (Figure 3a). This bilayer appeared to be homogeneous and had a diffusion coefficient of $1.6 \pm 0.5 \ \mu m^2 \ s^{-1}$. This rate is very similar to our measured diffusion coefficients on glass using the same lipid composition. If kept hydrated, these bilayers remained stable for up to 5 days. We note that the lower-temperature limit required to initiate bilayer formation has not been determined; however, incubation at 37 °C also resulted in uniform bilayer formation. This result has been observed on numerous samples, but interestingly, bilayer formation involved a two-stage process on at least one occasion. First, vesicle rupture/fusion occurred during the 50 °C incubation period, leading to the formation of

a double bilayer. The incomplete outer or uppermost bilayer displayed a rather lower diffusion coefficient of $0.7 \pm 0.2 \ \mu m^2 \ s^{-1}$ and an associated mobile fraction of 73% (Figure 3b). In the second stage, the uppermost bilayer disappeared during the 48 h incubation period and a more complete underlying bilayer was formed, which exhibited a diffusion coefficient of $1.0 \pm 0.02 \ \mu m^2 \ s^{-1}$ and a mobile fraction of 92% (Figure 3b). This bilayer-formation process was recorded as a video (Supporting Information, Figure S2). When the DOTAP concentration was increased to 50 mol %, a rather poor-quality lipid bilayer was formed with a diffusion coefficient of just $0.30 \pm 0.06 \ \mu m^2 \ s^{-1}$ and a mobile fraction of only 65%, even after extended incubation.

AFM images of the dry and hydrated PCysMA polymer brushes showed few surface features. The dry brushes had an rms roughness of 0.5 ± 0.2 nm, and the hydrated brush immersed in buffer had an rms roughness of 0.3 ± 0.1 nm. Figure 4a,b shows, respectively, a height image and surface profile obtained following bilayer formation on a PCysMA brush. Notably, there are few intact vesicles (∼20 nm feature sizes) visible on the surface. The breakthrough force curve shown in Figure 4c was obtained by applying sufficient force to the tip until it broke through the lipid layer. The bilayer depth indicated by this breakthrough force is 5 nm, which is consistent with the expected mean bilayer thickness. By scanning a reduced area using a relatively high applied force (3 nN), a 2 μm^2 area of lipid bilayer and the underlying PCysMA brush were scratched away (Figure 4d). The height profile across the edge of this area is 18 nm, which is close to the sum of the swollen brush thickness (12 nm) plus the bilayer thickness (5 nm). Figure 4g depicts the surface profile within
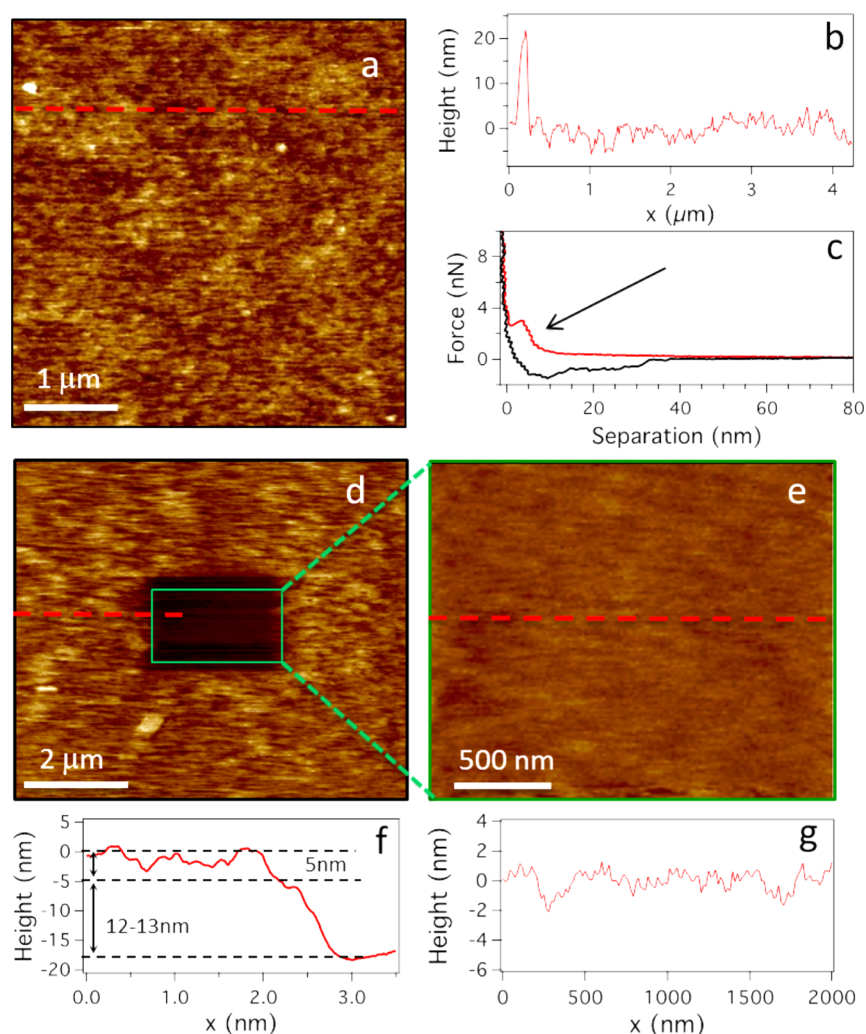
Figure 4. AFM images recorded following bilayer formation on a PCysMA brush: (a) height image; (b) height profile also showing a single adsorbed vesicle; (c) breakthrough force curve indicating a 5 nm bilayer thickness; (d) 2 μm^2 scratched region surrounded by a lipid bilayer on a PCysMA brush; (e) image at the base of the 2 μm^2 scratched area; (f) height profile across the bilayer/polymer scratch edge (position indicated by red dashed lines); and (g) height profile of the surface at the base of the scratched area.

Table 1. Results of Bilayer Formation on Four Polymer Brushes (Left Column) after Incubating with Vesicles of Different Lipid Composition (Top Row)[a]

		POPC	10% DOTAP	25% DOTAP	50% DOTAP
	zeta potential ± 5 (mV)	0	+25	+43	+64
PMPC	0	none	none	none	none
PCysMA	−10	none	none	bilayer $D > 1$	bilayer $0.1 < D > 0.9$
PKSPMA	−33	none	IV, $D \approx 0$	RM bilayer/V $D < 0.1$	RM bilayer/V, $D < 0.1$
PMAA	−43	none	IV, $D \approx 0$	RM bilayer/V, $D < 0.1$ ($0.3 < D^* < 0.8$)	bilayer/V, $D < 0.1$

[a]None signifies no or little vesicle adsorption. IV, immobile vesicles. Bilayer−bilayer has a characteristic diffusion coefficient similar to that of glass. RM bilayer, reduced-mobility bilayer. V, vesicle layer. Approximate diffusion coefficients, D, are given and have units of $\mu m^2\ s^{-1}$. The D^* value was obtained upon addition of 2 M NaCl.

this scratched area. The surface roughness within this scratched area is very close to that of bare glass.[54]

Bilayer Formation on PMAA and PKSPMA Brushes. Attempts to form bilayers on the anionic PMAA and PKSPMA brushes using DOTAP-containing vesicles combined with the incubation protocols described above did not yield mobile bilayers. Vesicles containing 10% DOTAP formed a layer of immobile vesicles and yielded inhomogeneous fluorescent images. Increasing the DOTAP molar ratio to 25 or 50 mol % led to more uniform fluorescent images, but only very low diffusion coefficients (<0.1 $\mu m^2\ s^{-1}$) were calculated from FRAP studies.

3673

■ DISCUSSION

Bilayer formation requires a driving force for vesicle adsorption, either through van der Waals forces or electrostatic interactions (or a combination of the two). If the interaction between the vesicles and the surface is too weak, then little or no vesicle adsorption is observed, as might be expected for neutral and zwitterionic surface/liposome combinations. Increasing the attractive vesicle/surface interaction leads to vesicle adsorption. If sufficient stress is induced in the vesicles during their interaction with the substrate, then they can undergo rupture and produce bilayer islands (if the vesicle surface coverage is low), which might ripen through interaction with freshly adsorbing vesicles or lipid or remain as isolated bilayer patches. Such behavior is associated with type 1 bilayer formation as described by Richter and Brisson.[55] If the vesicles interact less strongly with the substrate such that rupture does not spontaneously occur, then they remain intact and require an additional perturbation to induce rupture and fusion. This can be triggered by vesicle/vesicle interactions (and hence is favored at higher vesicle coverage) and is described as type II bilayer formation according to the nomenclature suggested by Richter et al.[55] Alternatively, an external trigger such as osmotic, temperature, ionic, or pressure stresses may be applied to initiate rupture.[56,68] After rupture, there is an energy penalty associated with exposed bilayer edges, providing a driving force for the fusion of ruptured vesicles, or membrane patches, into a full bilayer.[57−64]

The behavior of the polymer brushes examined in this study can be understood in light of electrostatic interactions, and Table 1 shows the various polymer brushes and liposome compositions arranged according to the magnitude of their zeta potentials. For pH values of between 3 and 8, the zwitterionic PMPC and PCysMA brushes exhibited only rather low zeta potentials of around 0 and −10 mV, respectively. The product of the zeta potential of the liposome and the polymer brush provides a useful guide regarding the strength of the electrostatic attraction, i.e., the driving force for vesicle adsorption/rupture. For zwitterionic POPC vesicles and zwitterionic brushes, the driving force for vesicle adsorption is clearly very weak, and hence bilayer formation is not observed. This is consistent with the observation of Vancso et al.,[31] who found that thicker PSBMA brushes did not support spontaneous vesicle adsorption/bilayer formation. It is also in agreement with Wirth's experiments on spin-coated PAM.[30]

By increasing the DOTAP concentration to 10%, the vesicle zeta potential increased up to +24 mV, which led to slightly higher vesicle coverage. However, this was insufficient to induce bilayer formation.

Importantly, by increasing the cationic content of the vesicles further (25:75 DOTAP/POPC; zeta potential = +45 mV) we were able to drive vesicle adsorption in the case of PCysMA but not in the case of PMPC. However, bilayer formation did not spontaneously occur but required an external stress. To induce vesicle rupture, the system was incubated above 50 °C for 1 h. (The lowest temperature required to induce vesicle rupture was not investigated, though the process still works at 37 °C.) This can be rationalized in light of the mechanism proposed by Kasemo et al., whereby the cationic lipids are attracted to anionic polymer brush chains while the zwitterionic lipids become rearranged around the rest of the vesicle.[65,66] With the intervesicle repulsion minimized, the vesicles can swell slightly at elevated temperature and hence induce rupture. These

conditions may initially create a partial double bilayer, which over prolonged incubation at room temperature evolved into a single bilayer.[67,68] Double bilayers have been proposed by Majewski et al., who studied PC vesicle interactions with PEI surfaces using neutron reflectivity. They suggested that their data were consistent with the formation of adsorbed vesicle layers and small regions of a double bilayer.[69] Furthermore, Han et al. observed double-bilayer formation and suggested that the outer bilayer was incomplete and only weakly connected to the proximal bilayer and hence might be easily removed.[70]

Increasing the DOTAP concentration to 50% (+60 mV) led to the strong electrostatic binding of vesicles. In the case of PCysMA brushes, these adsorbed vesicles rupture to form homogeneous bilayers but only relatively low diffusion coefficients ($D = 0.30 \pm 0.1$ μm^2 s^{-1}) and mobile fractions of ∼70% were observed, which might be due to the strong electrostatic interaction between DOTAP and the underlying support or might indicate the presence of intact vesicles/defects. These results suggest that electrostatic interaction is the principal mechanism for driving bilayer formation in the case of the PCysMA brush and is analogous to the electrostatics-driven bilayer formation previously observed by Cha et al., who systematically controlled the charge on the surface to show that a critical adsorbed vesicle concentration was required to cause bilayer formation (on both positively and negatively charged surfaces).[71] Interestingly, they also noticed that the nature of the buffer was also significant in influencing bilayer formation in the case of weaker electrostatic driving forces. Min et al. have recently monitored the zeta potential during bilayer formation to show that the transition between vesicle adsorption and bilayer formation is a first-order transition, which is consistent with the requirement to attain a critical vesicle concentration.[72] The PMPC brush, which incorporates both cationic (amine) and anionic (phosphate) groups, creates a zwitterionic moiety with a terminal tertiary amine. The surface zeta potential of the PMPC brush was ∼0 ± 10 mV, with little or no pH response. These surfaces were resistant to vesicle adsorption/bilayer formation irrespective of the nature of the liposome (e.g., whether anionic, cationic, or zwitterionic) or buffer conditions.

The PMAA and PKSPMA brushes have much higher negative zeta potentials (−43.2 ± 1.5 and −33.6 ± 2.3 mV, respectively). For the 10% DOTAP vesicles, these highly anionic brushes supported vesicle adsorption but not rupture or fusion. There was no evidence of any recovery following FRAP. For higher DOTAP concentrations on these surfaces, we observe homogeneous fluorescence, but it appears from FRAP studies that there is significant pinning of the charged lipid in the proximal leaflet of the bilayer, leading to reduced mobile fractions and diffusion coefficients. It is also possible that a uniform bilayer is not formed on the nanoscale but rather small patches of a highly charged bilayer. These might prohibit further vesicle adsorption due to electrostatic repulsion. Alternatively, it is possible that an adsorbed vesicle layer is formed, but vesicle−vesicle repulsion is sufficient to prevent this layer from becoming too dense, resulting in restricted vesicle motion and hence a reduced diffusion coefficient. Fischlechner et al.[36] also found that only a specific surface and lipid combination was successful, requiring a 50:50 mixture of zwitterionic and anionic lipid on a cationic polymer. They also found that more highly charged vesicles produced immobile vesicle layers. For the PMAA surface/25% DOTAP vesicle system, we have observed that by introducing 2 M NaCl

solution the diffusion coefficient increased to between 0.3 and 0.8 μm^2 s^{-1}. The explanation for this requires further investigation but might be associated with either the collapse of the brush to form a denser brush with a lower rms roughness, the introduction of electrostatic screening leading to a reduction in intervesicle repulsion, or a decrease in the lipid/surface interaction.

CONCLUSIONS

Our studies show the difficulty of predicting a priori the polymer/lipid properties required to form supported lipid bilayers on polymer brushes. Clearly, electrostatic interactions play a critical role in obtaining vesicle adsorption, rupture, and bilayer formation. Of the brushes examined, zwitterionic PMPC has a very low zeta potential and does not adsorb vesicles of any composition. The strongly anionic PMAA and PKSPMA brushes did support vesicle adsorption, albeit with very slow diffusion of intact vesicles or highly charged discontinuous bilayer patches. Although zwitterionic, the PCysMA brushes possess weakly negative zeta potentials which enable reproducible bilayer formation. In particular, the vesicle/brush interactions are optimized when using cationic vesicles prepared with 25% DOTAP. For this composition/surface combination, it is possible to form high-quality supported lipid bilayers that enable rapid diffusion and high mobile fractions. Work is ongoing to incorporate transmembrane proteins into this system, which involves the fusing of proteoliposomes with this preformed bilayer.

ASSOCIATED CONTENT

Ⓢ Supporting Information

^{1}H NMR studies on PCysMA, video of single-bilayer formation, and FRAP data for bilayer formation with a diffusion coefficient of 1.5 μm^2 s^{-1}. This material is available free of charge via the Internet at http://pubs.acs.org.

AUTHOR INFORMATION

Corresponding Author
*E-mail: s.d.evans@leeds.ac.uk.

Author Contributions

The manuscript was written using the contributions of all authors. All authors have given approval to the final version of the manuscript.

Notes

The authors declare no competing financial interest.

ACKNOWLEDGMENTS

REFERENCES

(1) McIntosh, T. J.; Simon, S. A. Roles of bilayer material properties in function and distribution of membrane proteins. *Annu. Rev. Biophys. Biomol. Struct.* **2006**, *35*, 177−198.

(2) de Planque, M. R.; Killian, J. A. Protein-lipid interactions studied with designed transmembrane peptides: role of hydrophobic matching and interfacial anchoring. *Mol. Membr. Biol.* **2003**, *20*, 271−284.

(3) Van Meer, G.; Voelker, D. R.; Feigenson, G. W. Membrane lipids: where they are and how they behave. *Nat. Rev. Mol. Cell Biol.* **2008**, *9*, 112−124.

(4) Phillips, R.; Ursell, T.; Wiggins, P.; Sens, P. Emerging roles for lipids in shaping membrane-protein function. *Nature* **2009**, *459*, 379−385.

(5) Brian, A. A.; McConnell, H. M. Allogeneic stimulation of cytotoxic T cells by supported planar membranes. *Proc. Natl. Acad. Sci. U.S.A.* **1984**, *81*, 6159−6163.

(6) McConnell, H.; Watts, T.; Weis, R.; Brian, A. Supported planar membranes in studies of cell-cell recognition in the immune system. *Biochim. Biophys. Acta* **1986**, *864*, 95−106.

(7) Tamm, L. K.; McConnell, H. M. Supported phospholipid bilayers. *Biophys. J.* **1985**, *47*, 105−113.

(8) Grieshaber, D.; MacKenzie, R.; Vörös, J.; Reimhult, E. Electrochemical biosensors-Sensor principles and architectures. *Sensors* **2008**, *8*, 1400−1458.

(9) Naumann, R.; Jonczyk, A.; Hampel, C.; Ringsdorf, H.; Knoll, W.; Bunjes, N.; Gräber, P. Coupling of proton translocation through ATPase incorporated into supported lipid bilayers to an electrochemical process. *Bioelectrochem. Bioenerg.* **1997**, *42*, 241−247.

(10) Richter, R. P.; Bérat, R.; Brisson, A. R. Formation of solid-supported lipid bilayers: an integrated view. *Langmuir* **2006**, *22*, 3497−3505.

(11) Cremer, P. S.; Boxer, S. G. Formation and spreading of lipid bilayers on planar glass supports. *J. Phys. Chem. B* **1999**, *103*, 2554−2559.

(12) Laschewsky, A.; Ringsdorf, H.; Schmidt, G.; Schneider, J. Self-organization of polymeric lipids with hydrophilic spacers in side groups and main chain: investigation in monolayers and multilayers. *J. Am. Chem. Soc.* **1987**, *109*, 788−796.

(13) Erbe, A.; Bushby, R. J.; Evans, S. D.; Jeuken, L. J. Tethered bilayer lipid membranes studied by simultaneous attenuated total reflectance infrared spectroscopy and electrochemical impedance spectroscopy. *J. Phys. Chem. B* **2007**, *111*, 3515−3524.

(14) Kendall, J. K.; Johnson, B. R.; Symonds, P. H.; Imperato, G.; Bushby, R. J.; Gwyer, J. D.; van Berkel, C.; Evans, S. D.; Jeuken, L. J. Effect of the structure of cholesterol-based tethered bilayer lipid membranes on ionophore activity. *ChemPhysChem* **2010**, *11*, 2191−2198.

(15) Raguse, B.; Braach-Maksvytis, V.; Cornell, B. A.; King, L. G.; Osman, P. D.; Pace, R. J.; Wieczorek, L. Tethered lipid bilayer membranes: formation and ionic reservoir characterization. *Langmuir* **1998**, *14*, 648−659.

(16) Sinner, E.-K.; Knoll, W. Functional tethered membranes. *Curr. Opin. Chem. Biol.* **2001**, *5*, 705−711.

(17) Terrettaz, S.; Mayer, M.; Vogel, H. Highly electrically insulating tethered lipid bilayers for probing the function of ion channel proteins. *Langmuir* **2003**, *19*, 5567−5569.

(18) Castellana, E. T.; Cremer, P. S. Solid supported lipid bilayers: From biophysical studies to sensor design. *Surf. Sci. Rep.* **2006**, *61*, 429−444.

(19) Sumino, A.; Dewa, T.; Takeuchi, T.; Sugiura, R.; Sasaki, N.; Misawa, N.; Tero, R.; Urisu, T.; Gardiner, A. T.; Cogdell, R. J.; Hashimoto, H.; Nango, M. Construction and structural analysis of tethered lipid bilayer containing photosynthetic antenna proteins for functional analysis. *Biomacromolecules* **2011**, *12*, 2850−2858.

(20) Giess, F.; Friedrich, M. G.; Heberle, J.; Naumann, R. L.; Knoll, W. The protein-tethered lipid bilayer: a novel mimic of the biological membrane. *Biophys. J.* **2004**, *87*, 3213−3220.

(21) White, R. J.; Zhang, B.; Daniel, S.; Tang, J. M.; Ervin, E. N.; Cremer, P. S.; White, H. S. Ionic conductivity of the aqueous layer separating a lipid bilayer membrane and a glass support. *Langmuir* **2006**, *22*, 10777−10783.

(22) Klapper, Y.; Vrânceanu, M.; Ishitsuka, Y.; Evans, D.; Scheider, D.; Nienhaus, G. U.; Leneweit, G. Surface energy of phospholipid bilayers and the correlation to their hydration. *J. Colloid Interface Sci.* **2013**, *390*, 267−274.

(23) Hwang, L. Y.; Götz, H.; Knoll, W.; Hawker, C. J.; Frank, C. W. Preparation and characterization of glycoacrylate-based polymer-tethered lipid bilayers on benzophenone-modified substrates. *Langmuir* **2008**, *24*, 14088−14098.

(24) Théato, P.; Zentel, R. Formation of lipid bilayers on a new amphiphilic polymer support. *Langmuir* **2000**, *16*, 1801−1805.

(25) Lin, Y.-H.; Minner, D. E.; Herring, V. L.; Naumann, C. A. Physisorbed polymer-tethered lipid bilayer with lipopolymer gradient. *Materials* **2012**, *5*, 2243−2257.

(26) Wagner, M. L.; Tamm, L. K. Tethered polymer-supported planar lipid bilayers for reconstitution of integral membrane proteins: silane-polyethyleneglycol-lipid as a cushion and covalent linker. *Biophys. J.* **2000**, *79*, 1400−1414.

(27) Mashaghi, S.; van Oijen, A. M. A versatile approach to the generation of fluid supported lipid bilayers and its applications. *Biotechnol. Bioeng.* **2014**, *111*, 2076−2081.

(28) Goennenwein, S.; Tanaka, M.; Hu, B.; Moroder, L.; Sackmann, E. Functional incorporation of integrins into solid supported membranes on ultrathin films of cellulose: impact on adhesion. *Biophys. J.* **2003**, *85*, 646−655.

(29) Elender, G.; Kühner, M.; Sackmann, E. Functionalisation of Si/SiO$_2$ and glass surfaces with ultrathin dextran films and deposition of lipid bilayers. *Biosens. Bioelectron.* **1996**, *11*, 565−577.

(30) Smith, E. A.; Coym, J. W.; Cowell, S. M.; Tokimoto, T.; Hruby, V. J.; Yamamura, H. I.; Wirth, M. J. Lipid bilayers on polyacrylamide brushes for inclusion of membrane proteins. *Langmuir* **2005**, *21*, 9644−9650.

(31) Santonicola, M. G.; Memesa, M.; Meszynska, A.; Ma, Y.; Vancso, G. J. Surface-grafted zwitterionic polymers as platforms for functional supported phospholipid membranes. *Soft Matter* **2012**, *8*, 1556−1562.

(32) Renner, L.; Pompe, T.; Lemaitre, R.; Drechsel, D.; Werner, C. Controlled enhancement of transmembrane enzyme activity in polymer cushioned supported bilayer membranes. *Soft Matter* **2010**, *6*, 5382−5389.

(33) El-khouri, R. J.; Bricarello, D. A.; Watkins, E. B.; Kim, C. Y.; Miller, C. E.; Patten, T. E.; Parikh, A. N.; Kuhl, T. L. pH responsive polymer cushions for probing membrane environment interactions. *Nano Lett.* **2011**, *11*, 2169−2172.

(34) Tang, Y.; Wang, Z.; Xiao, J.; Yang, S.; Wang, Y. J.; Tong, P. Studies of phospholipid vesicle deposition/transformation on a polymer surface by dissipative quartz crystal microbalance and atomic force microscopy. *J. Phys. Chem. B* **2009**, *113*, 14925−14933.

(35) Kaufmann, M.; Jia, Y.; Werner, C.; Pompe, T. Weakly coupled lipid bilayer membranes on multistimuli-responsive poly(n-isopropylacrylamide) copolymer cushions. *Langmuir* **2010**, *27*, 513−516.

(36) Fischlechner, M.; Zaulig, M.; Meyer, S.; Estrela-Lopis, I.; Cuéllar, L.; Irigoyen, J.; Pescador, P.; Brumen, M.; Messner, P.; Moya, S. Lipid layers on polyelectrolyte multilayer supports. *Soft Matter* **2008**, *4*, 2245−2258.

(37) Matyjaszewski, K.; Xia, J. H. Atom transfer radical polymerization. *Chem. Rev.* **2001**, *101*, 2921−2990.

(38) Cheng, N.; Brown, A. A.; Azzaroni, O.; Huck, W. T. S. Thickness-dependent properties of polyzwitterionic brushes. *Macromolecules* **2008**, *41*, 6317−6321.

(39) Rehfeldt, F.; Steitz, R.; Armes, S. P.; von Klitzing, R.; Gast, A. P.; Tanaka, M. Reversible activation of diblock copolymer monolayers at the interface by pH modulation, 2: membrane interactions at the solid/liquid interface. *J. Phys. Chem. B* **2006**, *110*, 9177−9182.

(40) Morse, A. J.; Edmondson, S.; Dupin, D.; Armes, S. P.; Zhang, Z.; Leggett, G. J.; Thompson, R. L.; Lewis, A. Biocompatible polymer brushes grown from model quartz fibres: synthesis, characterisation and in situ determination of frictional coefficient. *Soft Matter* **2010**, *6*, 1571−1579.

(41) Biesalski, M.; Johannsmann, D.; Rühe, J. Synthesis and swelling behavior of a weak polyacid brush. *J. Chem. Phys.* **2002**, *117*, 4988−4994.

(42) Ahmad, S. A.; Leggett, G. J.; Hucknall, A.; Chilkoti, A. Micro- and nanostructured poly [oligo (ethylene glycol) methacrylate] brushes grown from photopatterned halogen initiators by atom transfer radical polymerization. *Biointerphases* **2011**, *6*, 8−15.

(43) Santonicola, M. G.; Memesa, M.; Meszynska, A.; Ma, Y.; Vancso, G. J. Surface-grafted zwitterionic polymers as platforms for functional supported phospholipid membranes. *Soft Matter* **2012**, *8*, 1556−1562.

(44) Edmondson, S.; Nguyen, N. T.; Lewis, A. L.; Armes, S. P. Co-nonsolvency effects for surface-initiated poly (2-(methacryloyloxy) ethyl phosphorylcholine) brushes in alcohol/water mixtures. *Langmuir* **2010**, *26*, 7216−7226.

(45) Parnell, A. J.; Martin, S. J.; Jones, R. A.; Vasilev, C.; Crook, C. J.; Ryan, A. J. Direct visualization of the real time swelling and collapse of a poly (methacrylic acid) brush using atomic force microscopy. *Soft Matter* **2009**, *5*, 296−299.

(46) Alswieleh, A. M.; Cheng, N.; Canton, I.; Ustbas, B.; Xue, X.; Ladmiral, V.; Xia, S.; Ducker, R. E.; El Zubir, O.; Cartron, M. L. Zwitterionic Poly (amino acid methacrylate) Brushes. *J. Am. Chem. Soc.* **2014**, *136*, 9404−9413.

(47) Morse, A. J.; Edmondson, S.; Dupin, D.; Armes, S. P.; Zhang, Z.; Leggett, G. J.; Thompson, R. L.; Lewis, A. Biocompatible polymer brushes grown from model quartz fibres: synthesis, characterization and in situ determination of frictional coefficient. *Soft Matter* **2010**, *6*, 1571−1579.

(48) Axelrod, D.; Koppel, D. E.; Schlessinger, J.; Elson, E.; Webb, W. W. Mobility measurement by analysis of fluorescence photobleaching recovery kinetics. *Biophys. J.* **1976**, *16*, 1055−1069.

(49) Wilemski, G. On the derivation of Smoluchowski equations with corrections in the classical theory of Brownian motion. *J. Stat. Phys.* **1976**, *14*, 153−169.

(50) Alswieleh, A. M. M. Micro- and Nano-Structure of Polymers and Molecular Materials. Ph.D. Thesis, University of Sheffield, July 2014.

(51) Yu, S.; Chow, G. M. Carboxyl group (-CO2H) functionalized ferrimagnetic iron oxide nanoparticles for potential bio-applications. *J. Mater. Chem.* **2004**, *14*, 2781−2786.

(52) Semsarilar, M.; Ladmiral, V.; Blanazs, A.; Armes, S. Anionic polyelectrolyte-stabilized nanoparticles via raft aqueous dispersion polymerization. *Langmuir* **2012**, *28*, 914−922.

(53) Cho, N.-J.; Frank, C. W. Fabrication of a planar zwitterionic lipid bilayer on titanium oxide. *Langmuir* **2010**, *26*, 15706−15710.

(54) Takeda, S.; Yamamoto, K.; Hayasaka, Y.; Matsumoto, K. Surface OH group governing wettability of commercial glasses. *J. Non-Cryst. Solids* **1999**, *249*, 41−46.

(55) Richter, R.; Mukhopadhyay, A.; Brisson, A. Pathways of lipid vesicle deposition on solid surfaces: a combined QCM-D and AFM study. *Biophys. J.* **2003**, *85*, 3035−3047.

(56) Jackman, J. A.; Choi, J.-H.; Zhdanov, V. P.; Cho, N.-J. Influence of osmotic pressure on adhesion of lipid vesicles to solid supports. *Langmuir* **2013**, *29*, 11375−11384.

(57) Keller, C.; Kasemo, B. Surface specific kinetics of lipid vesicle adsorption measured with a quartz crystal microbalance. *Biophys. J.* **1998**, *75*, 1397−1402.

(58) Smith, A. M.; Vinchurkar, M.; Gronbech-Jensen, N.; Parikh, A. N. Order at the edge of the bilayer: Membrane remodeling at the edge of a planar supported bilayer is accompanied by a localized phase change. *J. Am. Chem. Soc.* **2010**, *132*, 9320−9327.

(59) Seifert, U.; Berndl, K.; Lipowsky, R. Shape transformations of vesicles: Phase diagram for spontaneous-curvature and bilayer-coupling models. *Phys. Rev. A* **1991**, *44*, 1182.

(60) Blount, M. J.; Miksis, M. J.; Davis, S. H. The equilibria of vesicles adhered to substrates by short-ranged potentials. *Proc. R. Soc. A* **2013**, *469*, 20120729.

(61) Rädler, J.; Strey, H.; Sackmann, E. Phenomenology and kinetics of lipid bilayer spreading on hydrophilic surfaces. *Langmuir* **1995**, *11*, 4539−4548.

(62) Nollert, P.; Kiefer, H.; Jähnig, F. Lipid vesicle adsorption versus formation of planar bilayers on solid surfaces. *Biophys. J.* **1995**, *69*, 1447−1455.

(63) Johnson, J. M.; Ha, T.; Chu, S.; Boxer, S. G. Early steps of supported bilayer formation probed by single vesicle fluorescence assays. *Biophys. J.* **2002**, *83*, 3371−3379.

(64) Zhdanov, V. P.; Dimitrievski, K.; Kasemo, B. Adsorption and spontaneous rupture of vesicles composed of two types of lipids. *Langmuir* **2006**, *22*, 3477−3480.

(65) Dimitrievski, K.; Kasemo, B. Simulations of lipid vesicle adsorption for different lipid mixtures. *Langmuir* **2008**, *24*, 4077−4091.

(66) Dimitrievski, K.; Kasemo, B. Influence of lipid vesicle composition and surface charge density on vesicle adsorption events: a kinetic phase diagram. *Langmuir* **2009**, *25*, 8865−8869.

(67) Wang, L.; Schönhoff, M.; Möhwald, H. Lipids coupled to polyelectrolyte multilayers: ultraslow diffusion and the dynamics of electrostatic interactions. *J. Phys. Chem. B* **2002**, *106*, 9135−9142.

(68) Reimhult, E.; Höök, F.; Kasemo, B. Intact vesicle adsorption and supported biomembrane formation from vesicles in solution: influence of surface chemistry, vesicle size, temperature, and osmotic pressure. *Langmuir* **2003**, *19*, 1681−1691.

(69) Wong, J. Y.; Majewski, J.; Seitz, M.; Park, C. K.; Israelachvili, J. N.; Smith, G. S. Polymer-cushioned bilayers. I. A structural study of various preparation methods using neutron reflectometry. *Biophys. J.* **1999**, *77*, 1445−1457.

(70) Han, X.; Achalkumar, A. S.; Cheetham, M. R.; Connell, S. D.; Johnson, B. R.; Bushby, R. J.; Evans, S. D. A self-assembly route for double bilayer lipid membrane formation. *ChemPhysChem* **2010**, *11*, 569−574.

(71) Cha, T.; Guo, A.; Zhu, X. Y. Formation of Supported Phospholipid Bilayers on Molecular Surfaces: Role of Surface Charge Density and Electrostatic Interaction. *Biophys. J.* **2006**, *90*, 1270−1274.

(72) Min, Y.; Pesika, N.; Zasadzinski, J.; Israelachvili, J. Studies of bilayers and vesicle adsorption to solid substrates: development of a miniature streaming potential apparatus (SPA). *Langmuir* **2010**, *26*, 8684−8689.